ELSEVIER

Physica A 251 (1998) 143–161

PHYSICA A

Fixed-node Monte Carlo calculations for the 1d Kondo lattice model

H.J.M. van Bemmel, W. van Saarloos *, D.F.B. ten Haaf

Instituut-Lorentz, Leiden University, P.O. Box 9506, 2300 RA Leiden, The Netherlands

Abstract

The effectiveness of the recently developed Fixed-Node Quantum Monte Carlo method for lattice fermions, developed by van Leeuwen and co-workers, is tested by applying it to the 1d Kondo lattice, an example of a one-dimensional model with a sign problem. The principles of this method and its implementation for the Kondo lattice model are discussed in detail. We compare the fixed-node upper bound for the ground-state energy at half filling with exact-diagonalization results from the literature, and determine several spin correlation functions. Our 'best estimates' for the ground-state correlation functions do not depend sensitively on the input trial wave function of the fixed-node projection, and are reasonably close to the exact values. We also calculate the spin gap of the model with the Fixed-Node Monte Carlo method. For this it is necessary to use a many-Slater-determinant trial state. The lowest-energy spin excitation is a running spin soliton with wave number π, in agreement with earlier calculations. © 1998 Elsevier Science B.V. All rights reserved.

PACS: 71.27.+a; 71.10.+x; 75.10.Jm; 71.20.Ad

Dedicated to Hans van Leeuwen on the occasion of his 65th birthday

1. Introduction

As is well known, quantum Monte Carlo simulations are plagued by the so-called sign problem [1,2]. The sign problem refers to the fact that when physical properties are sampled in configurations space, one collects large positive and negative contributions due to the fact that a fermion wave function is of different sign in different regions of configuration space. These contributions of opposite sign tend to cancel, giving results that may be exponentially smaller than the separate positive and negative contributions. Though the sign problem can be circumvented in special cases, e.g., for

* Corresponding author. E-mail: saarloos@lorentz.leidenuniv.nl.

PII S0378-4371(97)00601-8

the Hubbard model at half filling [3], no general solution has emerged yet from the various approaches that have been explored to cure it [4–10].

In 1990, when Alder was Lorentz Professor in Leiden, Hans van Leeuwen became acquinted with the Fixed Node Monte Carlo (FNMC) method of Ceperley and Alder [11–13], which avoids the sign problem in the context of continuum Green's function Monte Carlo. This stimulated him to explore the possibility of formulating a lattice version of FNMC, first with a postdoc, An [9], and later in collaborations with the present authors [10,14]. The formulation of the approach which was developed later [10] was shown to be variational [14], i.e. to give an upper bound to the exact ground state, and is the subject of this paper, which we dedicate to Hans van Leeuwen. We test this FNMC method for lattice fermions [10,14,15] on a simple one-dimensional (1d) model for which various results are available, the 1d Kondo lattice model (KLM) at half filling. This FNMC method involves an approximation that removes the sign problem in the context of Green's function Monte Carlo. Different Monte Carlo techniques that have been applied to the 1d KLM include the world-line algorithm [16], a finite temperature grand-canonical method involving a Hubbard–Stratonovich transformation [17,18] and the ground-state method developed by Sorella et al. [19,20]. All three Monte Carlo methods suffer from the sign problem, even in 1d.

The KLM is one of the basic models for correlated fermions. It can be obtained as the strong-coupling limit of the periodic Anderson model, which aims at capturing the essential physics of heavy-fermion materials [21–23]. In the limit of strong on-site repulsion among the f-electrons, a picture emerges of localized f-electrons interacting with a conduction band. In recent years, the model has been studied by a variety of methods, including variational approximations, exact diagonalizations and the density matrix renormalization group method [24–33]. This, together with the fact that quantum Monte Carlo simulations of this model do have a sign problem, makes the 1d KLM a suitable testing ground for our lattice FNMC method.

The lattice version of FNMC gives, like the continuum version [11–13,34] which inspired it, upper bounds for the ground state energy [14,35]. It improves upon a trial wave function for a given Hamiltonian by employing a Green's function projection method with a modified Hamiltonian in which all terms which would lead to unwanted sign changes in the sampling, are treated in a special way. The sign structure of the resulting approximate wave function, which is the ground state wave function of the modified Hamiltonian, is the same as that of the original trial wave. One obvious immediate question of interest is how close the FNMC energy estimate is to the exact ground-state energy of the original Hamiltonian. We will study this question by applying the fixed-node projection to a trial wave function with a free parameter. As we shall see, for the KLM, the ground-state energy obtained in the FNMC at half filling is quite independent of the precise trial wave, and quite close to the values obtained in exact diagonalization. We also compare the FNMC results for some correlation functions (which do not obey bounds), with exact results [29,20,36] for chains of six sites, with coupling constant J equal to 0.2 and 1.0. Here too we find that our best FNMC simulation estimates are rather independent of the starting trial wave function, and

reasonably close to the exact values. We finally also show how the spin gap of the 1d KLM can be determined with our FNMC, although this is computationally much more demanding, since a trial wave consisting of a sum of Slater determinants must be used. Good agreement is found with earlier results [32,33] in this case.

Before presenting our results, we first briefly discuss the 1d KLM and the reason why sampling it with unrestricted random walks leads to the sign problem. Then, in section Section 3, the principles of the lattice FNMC are summarized, followed by details of the implementation for the KLM. Section 4 gives the comparison with exact results for small lattices. In Section 5, our results for the running spin triplet excitation are discussed.

2. The Kondo lattice model

The Kondo lattice Hamiltonian is given by

$$\mathscr{H}_{\mathrm{KLM}} = -t \sum_{\langle ij \rangle} (c^{\dagger}_{i\sigma} c_{j\sigma} + c^{\dagger}_{j\sigma} c_{i\sigma}) - \mu \sum_{i} n_{ic} + J \sum_{i} \boldsymbol{S}_{if} \cdot \boldsymbol{S}_{ic} \,. \tag{1}$$

The two kinds of electrons, denoted by c for the conduction band and f for localized levels, have a spin–spin interaction. For the f's, the constraint is that there has to be precisely one f-electron on every site. In Eq. (1) and below, a summation convention is used for repeated spin indices.

We seek to write the Hamiltonian in a form that is convenient for GFMC calculations. If one would treat the f's as spins, which are not antisymmetrized but form a dynamical background for the conduction electrons, the total number of up-spin (and of down-spin) *fermions* would not be conserved by the Hamiltonian. It is not convenient to use this representation in a GFMC calculation whose starting trial wave is a fully fermionic mean-field-type wave function. If we use the constraint of one f-electron per site and the identities

$$\boldsymbol{S}_{if} = \tfrac{1}{2} f^{\dagger}_{i\sigma} \boldsymbol{\tau}_{\sigma\sigma'} f_{i\sigma'}, \qquad \boldsymbol{S}_{ic} = \tfrac{1}{2} c^{\dagger}_{i\sigma} \boldsymbol{\tau}_{\sigma\sigma'} c_{i\sigma'} \,, \tag{2}$$

where the components of $\boldsymbol{\tau}_{\sigma\sigma'}$ denote the three Pauli matrices, the Hamiltonian can be written in the form

$$\mathscr{H}_{\mathrm{KLM}} = -t \sum_{\langle ij \rangle} (c^{\dagger}_{i\sigma} c_{j\sigma} + c^{\dagger}_{j\sigma} c_{i\sigma}) - \frac{J}{2} \sum_{i} (c^{\dagger}_{i\sigma} f_{i\sigma})(f^{\dagger}_{i\sigma'} c_{i\sigma'}) - \mu' \sum_{i} n_{ic} \,, \tag{3}$$

with $\mu' = \mu - J/4$. This is now fully in fermionic language. Therefore, Slater determinants of fixed dimension can be used.

In many fermionic lattice models, e.g. the Hubbard model, the fermion statistics is not really important in Monte Carlo simulations in 1d. The reason is that, fermions of the same spin cannot pass each other in 1d and so their ordering is fixed. Since the exchanges that give rise to sign changes as a result of the fermion antisymmetry of the wave function are suppressed, there is no sign problem. In higher dimensions, this is not the case.

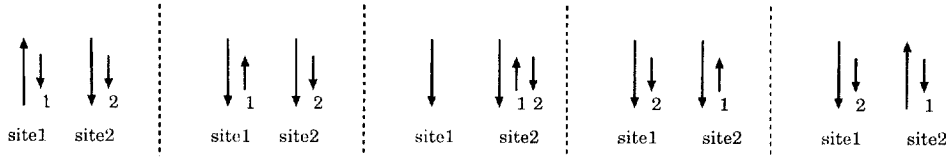

Fig. 1. A sequence of processes that lets two conduction electrons of equal spin pass each other in 1d. Large arrows denote f-electrons, small ones denote c-electrons. The successive states in the sequence are separated by vertical dashed lines.

For the 1d KLM, there is no fixed ordering of conduction electrons of equal spin. The presence of the spin flip term proportional to J in $\mathscr{H}_{\mathrm{KLM}}$ makes it possible for the ordering to change. This is illustrated in Fig. 1. A down c-electron at site 1 first changes in an up-electron, due to the simultaneous flip of a c-f pair. Then, the c-electrons at site 1 and 2 have opposite spins, so after a hop due to the kinetic term, they can occupy the same site. After an additional hop of the other c-electron, the two c-electrons then effectively have been interchanged.

Such an interchange can also happen in a Monte Carlo simulation, and one needs to take into account that two configurations that differ by the interchange of two numbered electrons must have opposite signs in the wave function. This is the reason why even the 1d KLM exhibits a sign problem [16,20]. In the case of 6 sites at half-filling with $J = 1.0$, which is studied by Otsuka [20], it appears that the sign problem is not very severe, but at certain filling fractions the sign problem is known to make simulations prohibitively difficult [16].

The 1d KLM has been studied in different regimes. If the number of f-electrons is equal to the number of sites, and the carrier concentration is low, there is a ferromagnetic state [26,27]. In weak coupling, at larger density but below half-filling, one obtains a paramagnetic state [28], and at half-filling, the system shows insulating spin-liquid behavior [17,30]. Recently, the ground state was proven to be a spin singlet and proven to be unique [37]. For slightly less than one f-electron per site, impurity bands arise [31].

In this paper, we limit ourselves to the case of half-filling, one c-electron per site. Finite-size scaling results [30] as well as recent density matrix renormalization group calculations [33] both show that there is a gap for spin and charge excitations for all $J > 0$ and thus confirm the insulating spin-liquid character of the ground state at half-filling.

3. The FNMC method for the KLM

3.1. Principles of the FNMC method

Since the general principles of the FNMC for lattice fermions have been laid out before [10,14,9], we only summarize the most essential aspects of the method here.

In a Green's function Monte Carlo method, one projects out the ground state of a system with Hamiltonian $\mathscr{H}$ from an initial trial state $|\psi_T\rangle$. As before [10,14,9], we use a projection operator $\mathscr{F}$ which acts as follows:

$$|\psi^n\rangle = \mathscr{F}^n |\psi_T\rangle = [1 - \tau(\mathscr{H} - w)]^n |\psi_T\rangle \ . \tag{4}$$

The implementation is in configuration space, and has a stochastic character. A specific configuration in configuration space, which determines the locations, spins, etc. of all the labeled electrons, is denoted by R, and we write $\psi_T(R) = \langle R \mid \psi_T\rangle$, etc. When τ is small enough and w adjusted properly during the sampling process [9,38], the operator $\mathscr{F}^n$ projects onto the ground state as $n \to \infty$. To obtain better statistics, we introduce *importance sampling*: we let the Green's function

$$G(R, R') = \psi_T(R) F(R, R') \psi_T^{-1}(R') \tag{5}$$

determine the transition probabilities of a random walker from R' to R; for simplicity, we take the trial wave function to be real. The projection (4) then becomes

$$\psi^n(R) = \sum_{R_n \cdots R_1} \psi_T(R) G(R, R_n) G(R_n, R_{n-1}) \cdots G(R_3, R_2) G(R_2, R_1) \psi_T^2(R_1) \ . \tag{6}$$

In the random-walk interpretation underlying the Monte Carlo process, the initial distribution of the random walkers is given by $\psi_T^2(R)$, and Eq. (6) is sampled stochastically by splitting G as

$$G(R, R') = P(R, R') m(R') \ , \tag{7}$$

with $m(R') \equiv \sum_R G(R, R')$ and hence $\sum_R P(R, R') = 1$. This notation anticipates that we wish to view P as a transition probability, the probability for a particle to make a transition from configuration R' to R, so that a path $R_1, R_2, \ldots, R_n$ in configuration space is generated by sampling the transitions according to P. The weight factors m which are accumulated along a path are sampled by viewing them as a multiplicity factor of each walker [9,38]. After a suitable number of steps, these multiplicity factors are sampled by a branching process: at these events, a walker with a multiplicity factor m can be either killed, stay alive, or split into more walkers in such a way that, on average, there are $\langle m \rangle$ new ones after the event. After each branching event, the factors m of all the walkers are reset to 1.

If all transition probabilities G would be positive, the above process could be implemented straightforwardly as in simulations of boson lattice models [38]. For fermions, the sign problem arises in the present formulation through the fact that $G(R, R')$, and hence $P(R, R')$, can be negative. In particular, for the KLM (3), as for the Hubbard model [10], all off-diagonal terms $\langle R | \mathscr{H}_{\mathrm{KLM}} | R' \rangle$ of the Hamiltonian $\mathscr{H}_{\mathrm{KLM}}$ are negative, and so negative signs arise in making transitions between configurations at which the trial wave function has opposite signs, $\psi_T(R)/\psi_T(R') < 0$. Taking those transition probabilities $P(R, R')$ proportional to $|G(R, R')|$ and carrying the sign with each walker would give positive and negative *multiplicities*, eventually, and therefore,

the implementation of Eq. (6) would lead to large positive and negative contributions to all measured quantities. The resulting cancellations are the essence of the sign problem.

In the lattice FNMC the sign problem is avoided by introducing a slightly different *effective Hamiltonian* $\mathscr{H}_{\text{eff}}$ in which all steps that lead to a sign change of the walker are left out, and replaced by a potential term [10,14]. The steps that are left out satisfy

$$\langle R|\mathscr{H}|R'\rangle\,\psi_{\text{T}}(R)\psi_{\text{T}}(R') > 0\,. \tag{8}$$

This is implemented by defining an effective Hamiltonian as follows: The off-diagonal terms are

$$\langle R|\mathscr{H}_{\text{eff}}|R'\rangle \equiv \begin{cases} \langle R|\mathscr{H}|R'\rangle & \text{if } \langle R|\mathscr{H}|R'\rangle\,\psi_{\text{T}}(R)\psi_{\text{T}}(R') < 0, \\ 0 & \text{otherwise,} \end{cases} \tag{9}$$

and the diagonal terms are

$$\langle R|\mathscr{H}_{\text{eff}}|R\rangle \equiv \langle R|\mathscr{H}|R\rangle + \langle R|\mathscr{V}_{\text{sf}}|R\rangle\,, \tag{10}$$

where the 'sign flip' potential that replaces the hops that satisfy Eq. (8) is given by

$$\langle R|\mathscr{V}_{\text{sf}}|R\rangle \equiv \sum_{R'}^{\text{sf}} \langle R|\mathscr{H}|R'\rangle\,\frac{\psi_{\text{T}}(R')}{\psi_{\text{T}}(R)}\,. \tag{11}$$

In this expression, the sum runs over all configurations R' connected by a non-zero matrix element $\langle R'|\mathscr{H}|R\rangle$ to the configurations R, for which Eq. (8) holds. The ground-state energy of $\mathscr{H}_{\text{eff}}$, which can be sampled without sign problem, gives [14] an upper bound to the ground-state energy of the true Hamiltonian $\mathscr{H}$. Expectation values of physical quantities are then obtained in the standard way [38,9].

3.2. The variational mean-field-type trial state for the KLM

As we saw above, a prerequisite for a Green's function Monte Carlo calculation is a trial wave function. For the KLM, we use what amounts to a Gutzwiller-projected mean-field-type wave function as a trial state. This wave function is essentially obtained as follows. Since earlier work indicates that this gives the lowest energy results, we use the Kondo decoupling scheme in Eq. (3), i.e., $\mathscr{H}_{\text{KLM}}$ is approximated by

$$\mathscr{H}_{V} = -t\sum_{\langle ij\rangle}(c^{\dagger}_{i\sigma}c_{j\sigma} + c^{\dagger}_{j\sigma}c_{i\sigma}) - \sum_{i}[(c^{\dagger}_{i\sigma}f_{i\sigma})V_i + (f^{\dagger}_{i\sigma'}c_{i\sigma'})V_i^{*}] - \frac{4}{J}\sum_{i}|V_i|^2\,. \tag{12}$$

The Hamiltonian $\mathscr{H}_V$ is bilinear in the fermion operators and hence can be diagonalized. We denote the ground state of this Hamiltonian by $|\psi_V\rangle$. The trial state $\langle\psi_{\text{T}}\rangle$ we use for our calculations is then

$$|\psi_{\text{T}}\rangle = P_{\text{G}}\,|\psi_V\rangle\,. \tag{13}$$

where P_G is the Gutzwiller projection operator which projects onto states in which each site is occupied by one f-electron [25,20].

For the homogeneous ground state, all V_i's should be taken equal, $V_i = V$. Following Otsuka [20], we will use this V as a variational parameter to construct a family of trial states for our ground-state calculations. The explicit form of the wave function can be easily obtained, and is given by Eq. (5) of Otsuka [20] (his parameter V is the same as ours). This wave function takes the form of a hybridized band state, but after Gutzwiller projection, it can also be written in the form of a overlapping Kondo cloud state [25].

We will actually find it more convenient to present our ground state results as a function of

$$b \equiv \langle \psi_{\Gamma'} | f_{i\sigma}^{\dagger} c_{i\sigma} | \psi_{\Gamma'} \rangle \,. \tag{14}$$

Note that the average is computed *before* Gutzwiller projection – in the Gutzwiller projected state the average is obviously zero. In the mean-field approximation, the self-consistency condition for the homogeneous ground state reads $Jb/2 = V$; this relation can easily be worked out in the thermodynamics limit, but as stated before, we will not use this.

We also use the Gutzwiller-projected mean-field solution as our trial state for the lowest-energy triplet state in Section 5. The mean-field solution in this case is inhomogeneous [32]; hence, in this case the parameters V_i in the selfconsistency conditions $J_i/2\langle \psi_{\Gamma'} | f_{i\sigma}^{\dagger} c_{i\sigma} | \psi_{\Gamma'} \rangle = V_i$ do depend on the spatial index i. We refer to the paper by Wang et al. [32] for a detailed discussion of the structure of this mean-field solution.

The single-particle levels of our trial wave are represented by an index for the energy level, an index for the site, and an index which indicates whether an electron has c or f character. This way of representing the trial wave function is suitable for the order in which the operators in the interaction term appear in Eq. (3), and for the decoupling we have chosen to generate the trial state. The operators between parentheses in the spin interaction term in $\mathcal{H}_{\mathrm{KLM}}$ represent intermediate steps in a Monte Carlo diffusion process. These correspond to changes within one spin sector. It is, therefore, natural to have numbered electrons of a certain spin and to allow changes from c to f and vice versa, rather than to have numbered electrons with the c or f character fixed and letting the spin change. Both representations are equivalent, but our choice allows to work with Slater-matrices of fixed size.

In the Monte Carlo calculation, the trial wave determines the distribution of random walkers; each walker represents a configuration, i.e., specifies the positions of each electron, its spin, and whether it is c or f. The weight of a certain configuration in the initial ensemble can be calculated from the trial state, by taking the product of the determinants corresponding to the spin-up and spin-down single-particle states. The ensemble is chosen by generating configurations at random, and then comparing the weight squared with a random number, in order to decide whether that configuration should be accepted as a member of the ensemble or not. By imposing the

constraint of one f-electron per site, the ensemble is automatically Gutzwiller-projected. Once the initial ensemble is Gutzwiller projected, the ensemble remains so during the projection process, since all moves allowed by $\mathscr{H}_{\mathrm{KLM}}$ keep the f-levels singly occupied.

3.3. Implementation of the FNMC for the KLM

For the KLM Hamiltonian Eq. (3), all off-diagonal terms $\langle R|\mathscr{H}|R\rangle$ are negative, for an antiferromagnetic spin-interaction $J > 0$. All steps are therefore according to Eq. (8) subdivided into allowed steps for which $\psi_{\mathrm{T}}(R)\psi_{\mathrm{T}}(R') > 0$ and forbidden steps for which $\psi_{\mathrm{T}}(R)\psi_{\mathrm{T}}(R') < 0$; the latter steps contribute to the sign flip potential [39] (11). If we use $\mathscr{H}_{\mathrm{KLM}}$ in the projector (4), three things can happen in one time step of the FNMC. First of all, R' can go to a configuration with one c-electron hopped to a neighboring position due to the kinetic term in $\mathscr{H}_{\mathrm{KLM}}$. The second possibility is a simultaneous spin flip: the spin interaction term proportional to J allows a configuration which has, on a certain site, a pair c-up, f-down, to change into c-down, f-up (or vice versa). The third possibility is that nothing happens in a time step: $R' = R$. The relative probabilities are given by Eq. (5). For a given walker, which corresponds to a given configuration, a list is therefore made of all possible allowed steps and their probabilities. When a forbidden step is encountered in making this list, the corresponding contribution to the sign-flip potential (11) is calculated. Since for every configuration R at most one electron changes its state (the site- or c/f label) per spin sector, the ratio $\psi_{\mathrm{T}}(R)/\psi_{\mathrm{T}}(R')$ which determines the probabilities and V_{sf}, can be calculated in a number of operations that is linear in the size of the system, if one already has the transposed inverse of the Slater matrices available [40].

Once an ensemble of random walkers with weight determined by the trial wave function has been prepared, as described in the previous subsection, the Monte Carlo projection is done according to Eq. (6). For a given walker, all possible moves are considered, and for each move, the ratio's $\psi_{\mathrm{T}}(R)/\psi_{\mathrm{T}}(R')$ are calculated. This operation corresponds to a dot product [40], so the time needed to compute it is linear in the system size. If $\psi_{\mathrm{T}}(R)/\psi_{\mathrm{T}}(R')$ is positive, the step to R is allowed. The probability factor $G(R,R') = P(R,R')m(R')$ of allowed Monte Carlo moves are stored in an ordered table in which each element is the sum of the previous element and the probability factor $\tau|\psi_{\mathrm{T}}(R)/\psi_{\mathrm{T}}(R')|$ for a hop or $J\tau|\psi_{\mathrm{T}}(R)/\psi_{\mathrm{T}}(R')|/2$ for a spin flip. The last element is the sum of the one but last element and the probability factor for staying, $G(R,R') = 1 - \tau(\mathscr{W}_{\mathrm{pot}} + \mathscr{V}_{\mathrm{sf}} - w)$, where $\mathscr{W}_{\mathrm{pot}} + \mathscr{V}_{\mathrm{sf}}$ is the total *potential* energy of $\mathscr{H}_{\mathrm{eff}}$. In this way, the value of the last element equals $\sum_R G(R,R') = m(R')$; the random decision to select a move or to stay is then made by deciding between which elements of the ordered table the product of a random number between 0 and 1 and $m(R')$ falls, using the Numerical Recipes routine *locate* [41].

The first stage of the diffusion implementation of the projection is a thermalization. During this stage, the parameter w in Eq. (4) $\mathscr{F} = 1 - \tau(\mathscr{H} - w)$ is adjusted in such a way that the ensemble of walkers stabilizes under the branching process by which the multiplicities of the walkers are updated; w approaches the measured ground state energy in this process. After the thermalization, the usual quantity being measured in a Green's function Monte Carlo is the *mixed estimator* $\langle\psi_T|\mathscr{O}|\psi^n\rangle$ for the *local value* of an operator $\mathscr{O}$,

$$O_{\text{local}}(R) = \langle R|\mathscr{O}|\psi_T\rangle / \psi_T(R) = \left[\sum_{R'} \langle R|\mathscr{O}|R'\rangle \langle R'|\psi_T\rangle\right] \Big/ \psi_T(R) . \tag{15}$$

The mixed-estimator is directly measured in the FNMC program, but a better estimate for an expectation value is obtained by assuming that the trial state is close to the ground state and neglecting quadratic terms in the difference [38]:

$$\langle\psi^n|\mathscr{O}|\psi^n\rangle \approx 2\langle\psi_T|\mathscr{O}|\psi^n\rangle - \langle\psi_T|\mathscr{O}|\psi_T\rangle . \tag{16}$$

We will refer to the right-hand side as the *best estimate*.

Operators which are diagonal, like the S_z spin correlation function are most efficiently calculated, since for off-diagonal terms computation of the ratio's $\psi_T(R')/\psi_T(R)$ takes substantial computer time. In our FNMC, τ needs to be small enough that $\mathscr{F}^n$ projects onto the ground state and large enough that the convergence is sufficiently rapid [9]. We typically work with an ensemble of on average $N_{\text{ens}} = 1000$ walkers. In one *interval*, all walkers are propagated during N_{time} time steps before branching. N_{time} is chosen such that the multiplicity factors m remain less than 2. After a thermalization of N_{therm} intervals, statistics is accumulated in N_{block} blocks of N_{intv} intervals each. In principle, the blocks are treated as independent measurements, and occasionally we check whether these are sufficiently independent indeed. If necessary, we increase N_{intv} to make them more independent; an example of this will be discussed in Section 5. The values of all these parameters used in the simulations will be listed in the figure captions.

4. Results for $J = 0.2$ and $J = 1.0$

As a first test of the FNMC on the KLM we compare with exact diagonalization results by Yamamoto and Ueda [29]. The coupling constant is $J = 0.2$, and the system consists of six sites with periodic boundary conditions. The trial wave functions we use are as described in Section 3.2.

In Fig. 2 we plot the FNMC energy as a function of b, defined in Eq. (14). Note that the energy estimates are above the exact ground-state energy, as they should be [14]. Furthermore, we see that the minimum is quite flat in the range $0.15 \lesssim b \lesssim 0.7$, and very close to the exact value (note the vertical scale!). Thus, our estimate for the ground-state energy one is quite independent of the trial wave function – apparently,

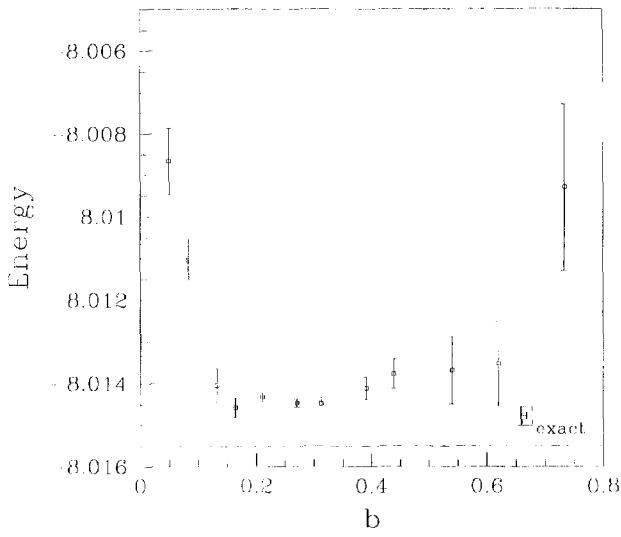

Fig. 2. Energy of a six-site KLM with $J = 0.2$; the parameters used in the Monte Carlo calculation are $\tau = 0.01$, $w_{\text{start}} = -8.3$, $N_{\text{time}} = 30$, $N_{\text{therm}} = 20$, $N_{\text{intv}} = 5$, $N_{\text{block}} = 400$, $N_{\text{ens}} = 1000$. The dashed horizontal line denotes the exact result of Yamamoto and Ueda [29].

therefore, while the variational energies do depend strongly on b, the projected energies are not very much affected by the fixed-node constraints over some range of values of b. Finally, also note that the statistical fluctuations are smaller close to the optimal value of b, $b \approx 0.25$, in agreement with the general trend that fluctuations are smaller the better the ground state is approximated, and that statistical fluctuations are reduced if there is a gap in the excitation spectrum [42] (the 1d KLM does have a gap).

An example of the mixed FNMC estimates of two spin correlation function, $\langle \psi_T | \boldsymbol{S}_c^i \cdot \boldsymbol{S}_c^i | \psi^n \rangle$ and $\langle \psi_T | \boldsymbol{S}_f^i \cdot \boldsymbol{S}_c^i | \psi^n \rangle$ for $J = 0.2$, are shown in Fig. 3. We see that near the optimal value of b, the mixed estimate is close to the exact value. At the same time, this figure illustrates that, not unexpectedly, the correlation functions are more sensitively dependent on the trial wave function than the projected energy shown in Fig. 2: at $b \approx 0.4$, the mixed estimate of the nearest neighbor c–f spin correlation function is almost a factor of 2 off, while the energy at this value is still quite close to the proper value. As we shall illustrate in detail below for $J = 1$, the estimates improve when we consider the best estimates instead.

For $J = 1.0$ we follow the same procedure as for $J = 0.2$ and compare with exact results obtained by Otsuka [20]. The upper line in Fig. 4a gives the energy measured in the *starting* ensemble, the lower line is the fixed-node value, i.e., after projection. Like in the case of $J = 0.2$, the latter curve is very flat, while the starting values depend strongly on the input wave function. Fig. 4b shows the same data on an expanded

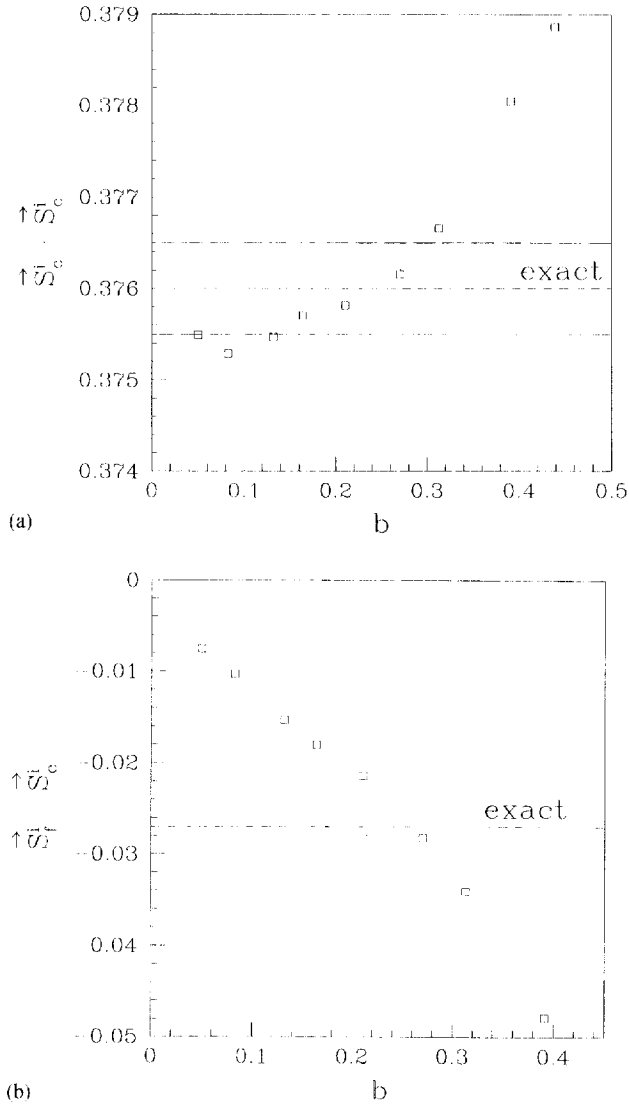

Fig. 3. Two examples of correlation functions in the $J = 0.2$ KLM. The parameters used in the FNMC program are $\tau = 0.03$, $w_{\text{start}} = -8.3$, $N_{\text{time}} = 30$, $N_{\text{therm}} = 20$, $N_{\text{intv}} = 5$, $N_{\text{block}} = 200$, $N_{\text{ens}} = 1000$. Only the mixed estimators are shown. The short dashed line indicates the exact value from Ref. [29], and the long dashed lines indicate the precision to which this exact result was given.

scale, on which one can see that the flat part of Fig. 4a really has a minimum. The exact diagonalization result [20] $E = -8.561616$ is also indicated in the picture. Clearly, also in this case the FNMC projection method is able to come quite close to the exact energy even if we start from a trial state that has a bad energy, and the statistical fluctuations are again smallest close to the minimum in FNMC energy.

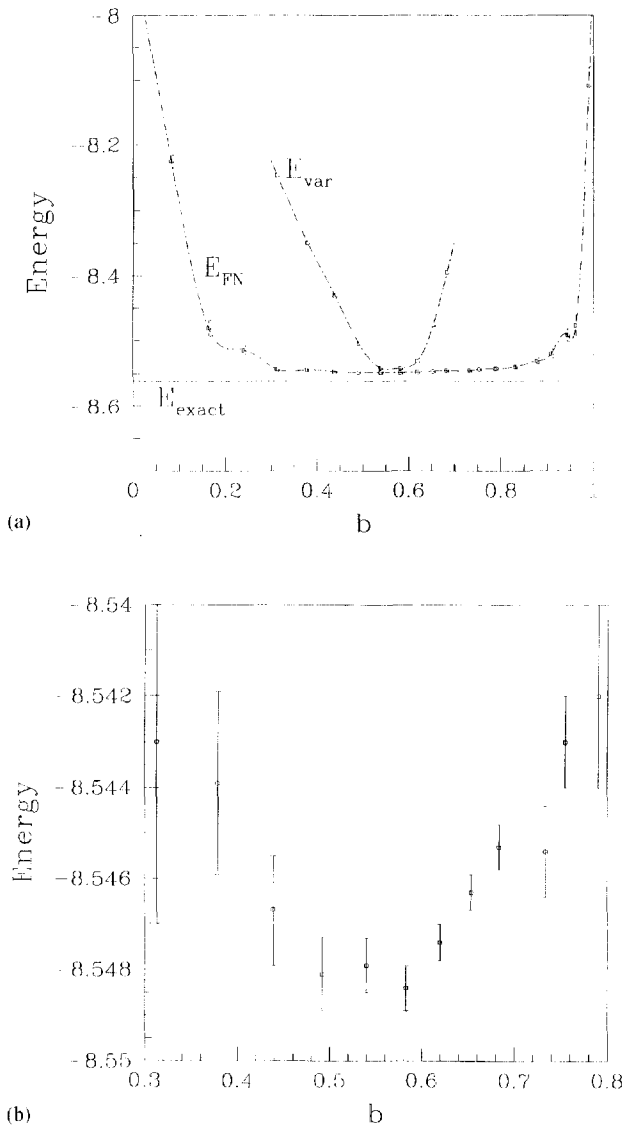

Fig. 4. Energy of a six-site KLM with $J = 1.0$; the parameters used in the FNMC calculation are $\tau = 0.003$, $w_{start} = -9.9$, $N_{time} = 20$, $N_{therm} = 20$, $N_{intv} = 1$, $N_{block} = 10\,000$, $N_{ens} = 1000$. In (b), the same results are plotted on an expanded scale.

In Figs. 5 and 6, we present the results for on-site correlation functions and correlation functions involving different sites, respectively. Three values are plotted: the variational value (using the Gutzwiller projected state $|\psi_V\rangle$), the mixed estimator and the best estimate given by Eq. (16). For all correlation functions considered, the latter

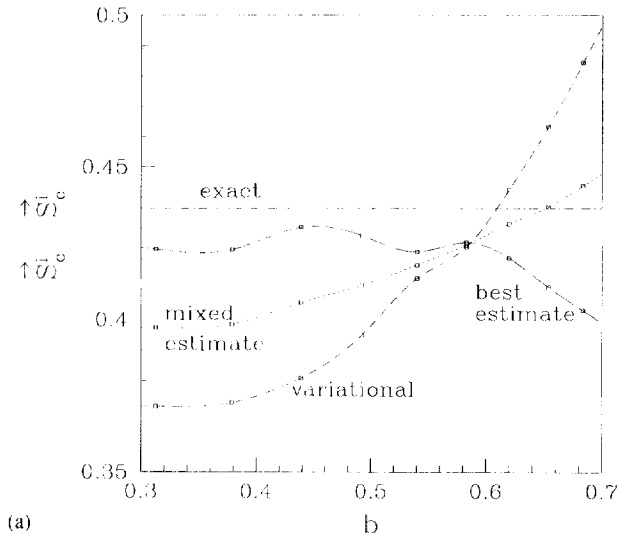

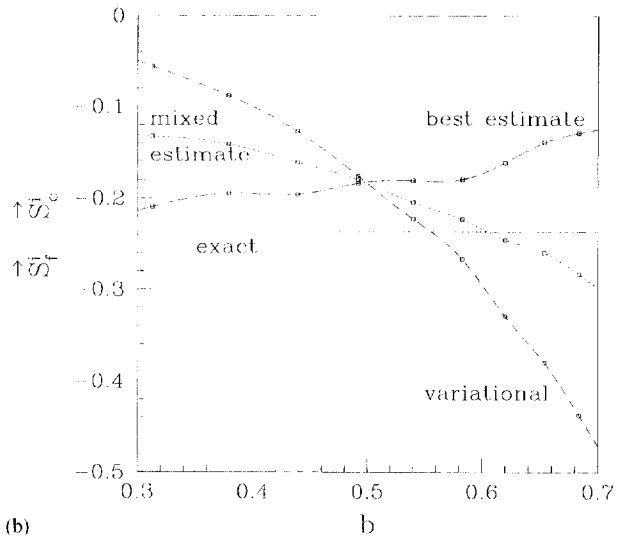

Fig. 5. On-site correlations in the $J = 1.0$ KLM. The parameters used in the FNMC calculation are $\tau = 0.003$, $w_{\text{start}} = -9.9$, $N_{\text{time}} = 20$, $N_{\text{therm}} = 20$, $N_{\text{mtx}} = 1$, $N_{\text{block}} = 200$, $N_{\text{ens}} = 1000$.

curve is relatively flat throughout the whole range of b values where the projected energy shown in Fig. 4 is close to the exact value. Thus, although the estimated correlations are slightly off, these results do show that, at least for the KLM, correlation functions are not strongly dependent on the trial state, and hence can be estimated relatively well with our FNMC.

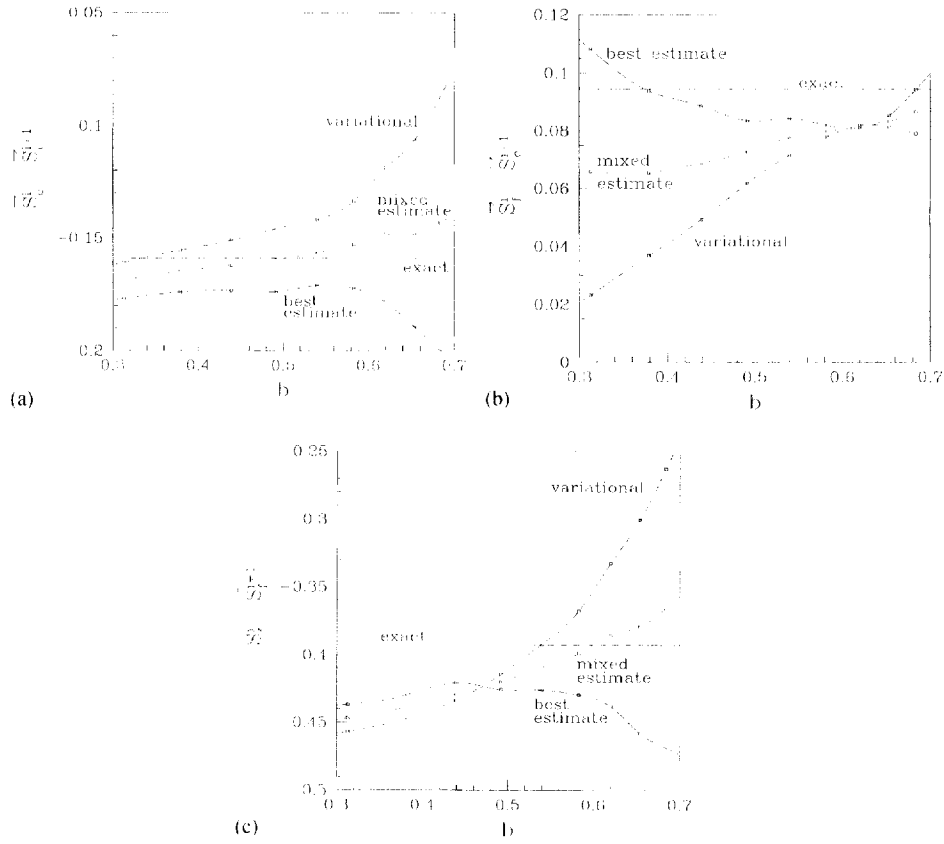

Fig. 6. Correlations on different sites in the $J = 1.0$ KLM. The parameters used in the FNMC calculation are $\tau = 0.003$, $w_{\text{start}} = -9.9$, $N_{\text{time}} = 20$, $N_{\text{therm}} = 20$, $N_{\text{intv}} = 1$, $N_{\text{block}} = 200$, $N_{\text{ens}} = 1000$.

5. FNMC calculation for the spin soliton

The lowest-energy excitation above the $S=0$ ground state of the half-filled KLM has total spin $S=1$ [32,33]. In a mean-field calculation, one is able to obtain a self-consistent solution with the spin excitation localized on a few sites [32]. Wang et al. [32] proceed by performing a Gutzwiller-projected mean-field calculation and by writing

$$|\psi_q\rangle = \sum_{x_c} \exp(iqx_c)\,|\psi_{x_c}\rangle, \tag{17}$$

with $|\psi_{x_c}\rangle = \mathscr{P}_G \left|\psi_{x_c}^{mf}\right\rangle$ the Gutzwiller-projected local triplet state with the center of the soliton located at x_c. The minimum of this dispersion is at wave number $q = \pi$. We follow the general strategy of investigating the robustness of mean-field results by using this wave function as trial wave function in a FNMC calculation. To obtain the spin-gap in the FNMC, we perform calculations both in the $S = 0$ and in the $S = 1$

sector. GFMC does not always project on the ground state, only on the lowest state that has a component along the trial-state. Here, we use this to our advantage: the total spin is conserved by the Hamiltonian, and, therefore, if one starts in the $S = 1$ sector, one remains in the $S = 1$ sector. Comparing the lowest energies in both sectors gives the gap.

Eq. (17) as it stands, seems to indicate that not only different *signs* occur, but also different complex *phases*. Because of reflection symmetry, however, one can combine q and $-q$ and write

$$|\psi_q\rangle = \sum_{x_c} \cos(qx_c)\,|\psi_{x_c}\rangle, \tag{18}$$

which is a real problem again [43].

We perform FNMC calculations for a system of 20 sites with periodic boundary conditions. This however takes computer time: for each possible step, 20 ratios of determinants need to be calculated, not just one, since

$$\frac{\psi_T(R)}{\psi_T(R')} = \frac{\sum_{x_c}\cos(qx_c)\langle R\,|\,\psi_{x_c}\rangle}{\sum_{x_c}\cos(qx_c)\langle R'\,|\,\psi_{x_c}\rangle} = \frac{\sum_{x_c}\cos(qx_c)\langle R'\,|\,\psi_{x_c}\rangle\,(\psi_{x_c}(R)/\psi_{x_c}(R'))}{\sum_{x_c}\cos(qx_c)\langle R'\,|\,\psi_{x_c}\rangle}. \tag{19}$$

The factors $\psi_{x_c}(R)/\psi_{x_c}(R')$ can be obtained as simple dot products again [40], in most cases. The exception is when $\psi_{x_c}(R') = 0$: in those cases $\psi_{x_c}(R)$ needs to be calculated from scratch, for which the computer time increases as the cube of the size of the system.

Note that this difficulty never occurs in a calculation with only one Slater determinant as trial wave function: with importance sampling, the probability to be in a configuration is proportional to $\psi_T(R')$, so if this is zero, a random walker never visits such a configuration. Therefore, we never need to compute ratios $\psi_T(R)/\psi_T(R')$ in which the *old* configuration R' has $\psi_{x_c}(R') = 0$. In the present case, only $\sum_{x_c}\cos(qx_c)\langle R'\,|\,\psi_{x_c}\rangle$ determines the probability to visit a configuration R', and a single $\psi_{x_c}(R')$ may be small or zero.

While smallness may be a practical difficulty in terms of numerical accuracy, the main problem is that a Slater-matrix can be really singular. In the case of a $S = 1$ soliton trial-state with $S_z = 1$, this turns out to happen for $\langle R'\,|\,\psi_{x_c}\rangle$ if the f-electron at site x_c has spin *down*, in configuration R', as is illustrated by the results of Fig. 2 of Wang et al. [32].

Considering possible moves, $\psi_{x_c}(R)$ needs to be calculated for all x_c and for all R. Computation of many values $\psi_{x_c}(R)$ from scratch would be very time-consuming. However, the only possibility to make a singular matrix non-singular, is to flip the spin of the f-electron (and of the c-electron) on site x_c. Such a flip can make one singular matrix non-singular, and *only* for the corresponding new configurations R do we need to calculate one Slater determinant.

In practice, we keep track of which of the 20 matrices are singular, for a certain random walker. For all hops, all non-zero new values $\psi_{x_c}(R)$ can be calculated as dot-products, so that in calculating the ratio (19) each flip in which one goes from f-down

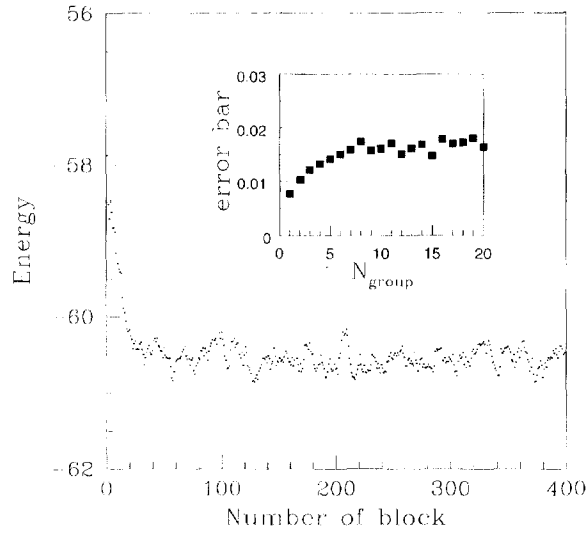

Fig. 7. Illustration of how a run proceeds: The average Monte Carlo energy calculated during one 'block' in the FNMC calculation for a $k = \pi$ soliton in a KLM on a 1d lattice of 20 sites with $J = 4.0$, calculated with parameters $\tau = 0.01$, $w_{\text{start}} = -90$, $N_{\text{therm}} = 3$, $N_{\text{time}} = 1$, $N_{\text{intv}} = 3$, $N_{\text{block}} = 400$, $N_{\text{ens}} = 200$. The inset shows the error bar of the last 300 blocks, and calculated by grouping N_{group} measurements together. For $N_{\text{group}} \gtrsim 3$, the error bars do not increase, indicating that the energies of different groups are statistically independent.

to f-up can make *one* Slater matrix non-singular, and for this one the determinant has to be calculated from scratch.

Once a step has been chosen, all matrices have to be updated. If it is a flip from f-up to f-down, one determinant becomes singular. If it is a flip with f-down to f-up, one matrix becomes non-singular, and its transposed inverse needs to be calculated, for facilitating the calculation of transition probabilities of subsequent steps. Except for this more complicated calculation of $\psi_{\text{T}}(R)/\psi_{\text{T}}(R')$, the FNMC program is the same as described before.

Fig. 7 illustrates how the FNMC projection proceeds as the number of iterations increases. First, one observes projection on the ground state: the energy measured over a number of Monte Carlo time steps, a 'block', drops. Then, there are fluctuations around a mean value. Accumulating statistics leads to a reduction of the error bars. One observes that the measurements in consecutive blocks are not independent. The correct error bar is obtained by grouping N_{group} measurements together and thus dividing the N_{total} blocks in $N_{\text{total}}/N_{\text{group}}$ measurements. After this regrouping, one has fewer values, but they are more independent. The error bars this gives are plotted in the inset of Fig. 7: the value of the plateau is the error bar we report in the energy dispersion curve (all error bars in energies are obtained this way).

The FNMC dispersion of the spin soliton, for $J = 4.0$, on 20 sites, is presented in Fig. 8. Since the $S = 0$ value is $E_{S=0}^{\text{FNMC}} = -63.423(5)$, and the minimum of the dispersion is at $E_{S=1}^{\text{FNMC}} = -60.47(3)$, the gap we obtain in FNMC approximation is

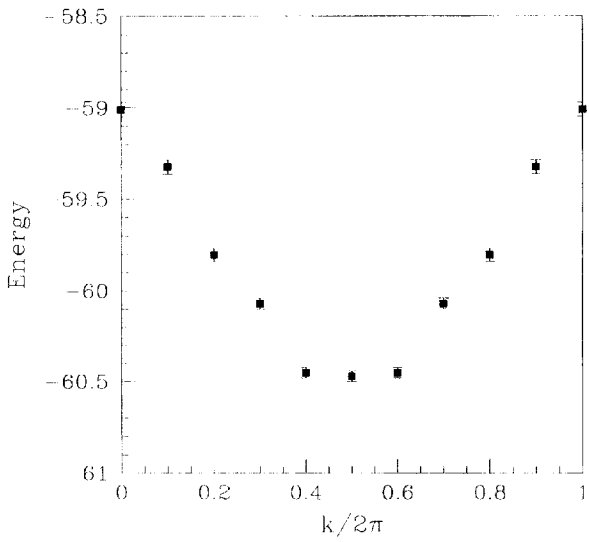

Fig. 8. Dispersion of a running soliton in a $J = 4.0$ KLM of 20 sites. The parameters used in the Monte Carlo calculations are $\tau = 0.005$, $w_{\text{start}} = -90$, $N_{\text{time}} = 1$, $N_{\text{therm}} = 3$, $N_{\text{intv}} = 3$, $N_{\text{block}} = 200$, $N_{\text{ens}} = 200$.

$\Delta_S^{\text{FNMC}} = 2.95(3)$, which is in agreement with the results shown in Fig. 3 of Wang et al. using a Gutzwiller-projected mean-field approximation, and those of Yu and White [33] using the density matrix renormalization group method. So, while the energies in both the $S = 0$ and the $S = 1$ sector drop relative to the one estimated with the Gutzwiller-projected mean-field wave function, the *difference* between the $S = 0$ and the $S = 1$ ground state energies is essentially the same as what is known to be the correct value [33].

6. Conclusions

We have applied the lattice FNMC method to the 1d KLM. We observe that, for small lattices, quite accurate ground-state energy estimates are obtained, even if the starting trial wave function gives quite a bad approximation to the energy. In the FNMC, the energy estimate is always above the exact ground state energy, but in the cases studied here, they are only slightly above the exact values for a large range of values in the variational trial wave. Over the same range over which a good ground-state energy estimate is obtained, reasonably accurate values for correlation functions in FNMC approximation are obtained, which again are rather independent of the starting trial-state of the KLM. To be able to calculate a dispersion of an excitation, one needs a conserved quantity, such that the lowest energies in different sectors can be compared – e.g., the isospin gap [33] of the KLM can not be obtained within our FNMC, but the spin-gap can, since for its determination only ground-state energies of

different spin sectors are needed. If inversion symmetry is present, one does not need to use complex phases and the FNMC method for a real wave function can be applied.

In the present case, therefore, the FNMC appears to work well, in that the constraint imposed by the fixed node condition do not appear to have a dramatic effect on the energies and correlation functions over a reasonably large range of values of b. Unfortunately, as long as we lack more fundamental insight in the sign structure of the fermion wave function, it is difficult to say whether this is just one lucky example, or a robust property. Of course, in the present case our trial wave function has properly built in the tendency of the c and f-spins to form singlets, and our fixed-node estimates are not good in the extreme limits $b \to 0$ (no local singlet correlations) and $b \to 1$ (tightly bound singlets).

For the smaller lattice sizes we have considered here, the sign problem does not appear to be so severe [20], but for the larger lattice sizes, like those needed to study the spin triplet excitation or domain walls in the two-dimensional Hubbard model [10], the advantages of the FNMC are more prominent.

Our results also throw new light on our own earlier results for domain walls in the two-dimensional Hubbard model [10]. In these simulations, we compared ground state energies starting from a homogeneous trial state and from a domain wall trial state. Although the lowest energy state was found when applying a FNMC projection to a domain wall trial state, the ground state energy obtained after FNMC projection of a homogeneous trial state was found to be relatively close. Since it is conceivable that, e.g., domain-wall-type correlations do build up during the projection of a homogeneous trial state, a study of the correlation functions is needed before clear conclusions can be drawn.

Acknowledgements

We are grateful to P.J.H. Denteneer for illuminating discussions and in particular to J.M.J. van Leeuwen for introducing us to the subject and for discussions and advice.

References

[1] H. De Raedt, W. von der Linden, in: K. Binder (Ed.), The Monte Carlo Method in Condensed Matter Physics, Springer, Berlin, 1992.
[2] M. Suzuki, Physica A 194 (1993) 432.
[3] J.E. Hirsch, Phys. Rev. B 31 (1985) 4403.
[4] M. Boninsegni, E. Manousakis, Phys. Rev. B 46 (1990) 560.
[5] E.Y. Loh, J.E. Gubernatis, R.T. Scalettar, S.R. White, D.J. Scalapino, R.J. Sugar, Phys. Rev. B 41 (1990) 9301.
[6] S. Sorella, S. Baroni, R. Car, M. Parrinello, Europhys. Lett. 8 (1989) 663.
[7] S. Fahy, D.R. Hamann, Phys. Rev. B 43 (1991) 765.
[8] S. Zhang, J. Carlson, J.E. Gubernatis, Phys. Rev. Lett. 74 (1995) 3652.
[9] G. An, J.M.J. van Leeuwen, Phys. Rev. B 44 (1991) 9410.
[10] H.J.M. van Bemmel, D.F.B. ten Haaf, W. van Saarloos, J.M.J. van Leeuwen, G. An, Phys. Rev. Lett. 72 (1994) 2442.

[11] D.M. Ceperley, B.J. Alder, Phys. Rev. Lett. 45 (1980) 566.
[12] D.M. Ceperley, B.J. Alder, Science 231 (1986) 555.
[13] P.J. Reynolds, D.M. Ceperley, B.J. Alder, W.A. Lester, Jr., J. Chem. Phys. 77 (1982) 5593.
[14] D.F.B. ten Haaf, H.J.M. van Bemmel, J.M.J. van Leeuwen, W. van Saarloos, D.M. Ceperley, Phys. Rev. B 51 (1995) 13039.
[15] The FNMC of Refs.[10,11] is based in spirit on the approach developed in Ref.[9], but this earlier formulation did not lead to an upper bound on the ground state energy.
[16] M. Troyer, D. Würtz, Phys. Rev. B 47 (1993) 2886.
[17] R.M. Fye, D.J. Scalapino, Phys. Rev. Lett. 65 (1990) 3177.
[18] R.M. Fye, D.J. Scalapino, Phys. Rev. B 44 (1991) 7486.
[19] S. Sorella, E. Tosatti, S. Baroni, R. Car, M. Parrinello, Int. J. Mod. Phys. B 1 (1988) 993.
[20] H. Otsuka, Phys. Rev. B 49 (1994) 1557.
[21] See, e.g., P.A. Lee, T.M. Rice, J.W. Serene, L.J. Sham, J.W. Wilkins, Comments Condens. Matter Phys. 12 (1986) 99.
[22] G. Aeppli, Z. Fisk, Comments Condens. Matter Phys. 16 (1992) 155.
[23] A.C. Hewson, The Kondo Problem to Heavy Fermions,, Cambridge University Press, Cambridge, 1993.
[24] C. Lacroix, M. Cyrot, Phys. Rev. B. 20 (1979) 1969.
[25] H. Shiba, P. Fazekas, Prog. Theor. Phys. (Suppl.) 101 (1990) 403.
[26] P. Fazekas, E. Müller-Hartmann, Z. Phys. B 85 (1991) 285.
[27] M. Sigrist, K. Ueda, H. Tsunetsugu, Phys. Rev. B 46 (1992) 175.
[28] For a summary of what is known of the phase diagram of the 1d KLM off half-filling, see e.g. K. Ueda, T. Nishino, H. Tsunetsugu, Phys. Rev. B 50 (1994) 612.
[29] K. Yamamoto, K. Ueda, J. Phys. Soc. Japan 59 (1990) 3284.
[30] H. Tsunetsugu, Y. Hatsugai, K. Ueda, M. Sigrist, Phys. Rev. B 46 (1992) 3175.
[31] P. Schlottmann, Phys. Rev. B 46 (1992) 998.
[32] Z. Wang, X.-P. Li, D.H. Lee, Phys. Rev. B 47 (1993) 11935.
[33] C.C. Yu, S.R. White, Phys. Rev. Lett. 71 (1993) 3866.
[34] G. Ortiz, D.M. Ceperley, R.M. Martin, Phys. Rev. Lett. 71 (1993) 2777.
[35] The name 'fixed-node' is actually a slight misnomer for our method, since the nodes of a wave function are not always properly defined for a discrete configuration space. In our method, the domains where the trial wave has a given sign are held fixed.
[36] The sizes for which exact-diagonalization results exist are rather small, because the size of the Fock space is 8^N, with N the number of sites.
[37] H. Tsunetsugu, Phys. Rev. B. 55 (1997) 3042.
[38] N. Trivedi, D.M. Ceperley, Phys. Rev. B. 41 (1990) 4552.
[39] Because in this case the sign flip in Eq. (8) always corresponds to a change in sign of the trial wave function, the sign flip potential V_{sf} is the same as the 'nodal boundary potential' used before [10]; the term sign flip potential introduced later [14] is more widely applicable.
[40] D.M. Ceperley, M.H. Kalos, Phys. Rev. B 16 (1977) 3081.
[41] W.H. Press, B.P. Flannery, S.A. Teukolsky, W.T. Vetterling, Numerical Recipes., Cambridge University Press, Cambridge, 1986.
[42] See, e.g., S. Goedecker, K. Mashke, Phys. Rev. B 44 (1991) 10365.
[43] For further discussion of the problems concerning complex lattice problems and possible generalizations of the fixed-node method we refer to H.J.M. van Bemmel, Thesis, Leiden University, 1995 (available from the authors).